Journal of Biomedical Optics

SPIEDigitalLibrary.org/jbo

Noninvasive and label-free determination of virus infected cells by Raman spectroscopy

Kamila Moor
Kiyoshi Ohtani
Diyas Myrzakozha
Orik Zhanserkenova
Bibin. B. Andriana
Hidetoshi Sato

SPIE

Noninvasive and label-free determination of virus infected cells by Raman spectroscopy

Kamila Moor,[a] Kiyoshi Ohtani,[a] Diyas Myrzakozha,[b] Orik Zhanserkenova,[b] Bibin. B. Andriana,[a] and Hidetoshi Sato[a,*]
[a]Kwansei Gakuin University, School of Science and Technology, Department of Bioscience, 2-1 Gakuen, Sanda, Hyogo 669-1337 Japan
[b]Kazakh National Agrarian University, Kazakhstan-Japan Innovation Centre, 8, Abai Street, Almaty 050010, Kazakhstan

Abstract. The present study demonstrates that Raman spectroscopy is a powerful tool for the detection of virus-infected cells. Adenovirus infection of human embryonic kidney 293 cells was successfully detected at 12, 24, and 48 h after initiating the infection. The score plot of principal component analysis discriminated the spectra of the infected cells from those of the control cells. The viral infection was confirmed by the conventional immunostaining method performed 24 h after the infection. The newly developed method provides a fast and label-free means for the detection of virus-infected cells. [DOI: 10.1117/1.JBO.19.6.067003]

Keywords: Raman spectroscopy; virus; cells.

Paper 140052RR received Jan. 28, 2014; revised manuscript received May 12, 2014; accepted for publication May 13, 2014; published online Jun. 4, 2014.

1 Introduction

Raman spectroscopy is a promising technique for the analysis of biomedical samples. The use of the Raman microscope enabled direct measurements of single-live cells. During the past few decades, Raman spectroscopy has been used for bacterial identification. Using Raman spectroscopy, Kastanos et al.[1] identified various strains of bacteria found in urinary tract infections: 25 strains of *Escherichia coli*, 25 strains of *Klebsiella pneumonia*, and 25 strains of *Proteus spp*. Raman spectroscopy is also used for identification of mycobacterium.[2] The previous studies have demonstrated that the Raman spectroscopy provides sufficient information to identify specific micro-organisms.[3–5] Raman spectroscopy has also been applied to the analysis of cells. Notingher et al.[6] used a Raman microspectrometer to characterize living cells attached to bioinert silica materials. Oshima et al.[7] measured Raman spectra of single-live human lung cancer cells and successfully discriminated them by multivariate analysis. Hartmann et al.[8] studied the effects of an anticancer drug by Raman spectroscopy and observed changes in DNA/RNA and proteins. Earlier studies revealed that even minor alterations that occur in living cells could be detected using Raman spectroscopy in a totally noninvasive and label-free manner. The Raman spectroscopy has also been used to study the structures of proteins, nucleic acids, and other components of virus, including conformational changes during viral procapsid and capsid assembly.[9,10] Viral infections lead to many diseases, including certain forms of cancers.[11–13] Recombinant viruses can be fluorescently labeled, e.g., with green fluorescent protein, to allow for the detection of infected cells in *in vitro* studies. Alternatively, immunostaining can also be used for their detection.[14,15] However, these conventional methods are effective only if the type of virus under investigation is known in advance. Therefore, we cannot detect an unknown virus even if it has human infectability. We can confirm the existence of the human infecting virus only when a person has been infected by it. Thereby, development of new techniques for the identification of pathogenic viruses is highly desirable.

The purpose of the present study was to examine the viability of Raman spectroscopy for the label-free detection and discrimination of virus-infected cells in a very early stage. Hamden et al.[16] succeeded in discriminating BCBL-1 and BC-1 cells, which were infected with Kaposi's sarcoma-associated herpesvirus (KSHV) from BJAB cell without KSHV by using Raman tweezers. They were cultured cells in which the virus gene was already recombined. Jess et al.[17] suggested that the Raman spectroscopy and principal component analysis (PCA) could discriminate primary human keratinocytes (PHK), PHK expressing the E7 gene of human papillomavirus (HPV), and HPV-containing cervical carcinoma derived cell line. These previous reports showed that the Raman spectroscopy was able to distinguish the cells in which the viral gene had already been fully expressed but did not describe the detection in the early stage of the viral infections.

To study the early stage of the virus infection, we employed a recombinant adenovirus that lacks the E1 geneand human embryonic kidney 293 (HEK293) cells harboring this factor. Since the E1 factor was necessary for reproduction of the virus, this virus cannot proliferate in normal human cells that lack this factor, making the present study safe.[18,19]

2 Experiment

2.1 *Preparation and Culture of Virus-Infected Cells*

Human embryonic kidney epithelial (HEK293) cells were purchased from DS Pharma Biomedical (Japan). The HEK293 cells were cultured in high-glucose Dulbecco's Modified Eagle Medium (DMEM; WAKO, Japan) supplemented with 10% fetal bovine serum (FBS; Beit HAEMEK, LTD., Israel) and 100 IU/mL penicillin (WAKO, Japan). The cells were maintained at 37°C and 5% CO_2 in a humidified incubator. A special dish with a quartz window at the bottom purchased from

*Address all correspondence to: Hidetoshi Sato, E-mail: hidesato@kwansei.ac.jp

Synapse-Gibko (Japan) was used for Raman measurements. Adenovirus (Ad-CMV-control) stock was prepared according to the reported methods.[18] The virus was stored at −80°C until use. The viral titer used was 0.5×10^6 PFU/mL, and the multiplicity of infection (MOI) was 6 PFU/cell. The viral infection was confirmed by immunostaining. A rabbit polyclonal antibody (anti-72K Ab) was employed, which detected the E2 polypeptide of the adenovirus. For fluorescence imaging, a fluorescein isothiocyanate (FITC)-labeled antibody, which detected rabbit IgGs, was used. The fluorescent images were captured using a Nikon A-1 (Nikon, Japan) confocal fluorescence microscope.

2.2 *Raman Measurements*

Raman measurements were made using a confocal Raman microscope (Nanofinder, Tokyo Instruments, Japan). The system had a CO_2 incubator, which maintained the culture dishes at 37°C in an atmosphere of 5% CO_2 during the measurements (Fig. 1). A continuous wave background-free electronically tuned Ti:sapphire laser (CW-BF-ETL; Mega Opto, Japan) provided an excitation beam of 785-nm wavelength. The laser power was typically set to 30 mW during sampling. The exposure time was 30 s × 3 times. The microscope was equipped with a ×60 water-immersion objective lens (NA = 1, 10, Olympus, Japan), a Raman polychromator equipped with a grating (600 1/mm, 750 nm-blazed), and a Peltier-cooled CCD detector (DU-401-BR-DD, Andor Technology, Ireland). The spectral resolution was 5 cm^{-1}. The measurements were made 12, 24, and 48 h after the addition of the virus. To measure the spectra, the laser was focused into the nucleus of the cells. The spectra were collected from approximately 12 randomly selected cells in each dish. The spectrum of the cell was processed by background subtraction and sixth polynomial fitting to remove the artifacts from the culturing media and the dish window. Some of the spectra which had very low signal because of instrumental disorder were removed from the dataset.

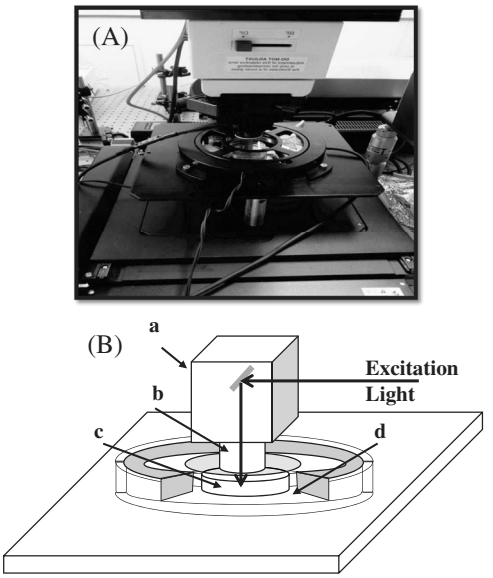

Fig. 1 Photograph (A) and scheme (B) of sampling stage of Raman microscope. The stage consists of microscope (a), objective lens (b), culturing dish (c), and indium tin oxide glass heater (d).

The Raman spectra of cells were processed by PCA. The intensities of the spectra were normalized using a band at 1003 cm^{-1} of phenylalanine or a band at 1440 cm^{-1} assigned to a CH deformation mode. Multivariate analysis software, Unscrambler (CAMO, Norway), was used for further analysis. The data were mean centered before the PCA. The results for the dataset normalized with the phenylalanine band is very similar to that normalized with the CH deformation band in PCA score plots. Therefore, we discuss the results of the dataset normalized with phenylalanine band in Sec. 3.

3 Results and Discussion

Microscopic images of HEK293 cells without (a) and with (b) virus after 48 h of cultivation are shown in Figs. 2(a) and 2(b). The density of the cells appears different in the images, but it is unrelated to the virus. Quinlan and Grodzicker reported that the adenovirus starts proliferating in the cells within 12 h.[19] However, viral infection could not be assessed by observing the morphological changes of the cells, and no apparent changes in morphology were observed during infection. Apoptotic or necrotic cells were not found when examined 48 h after the addition of the virus. Figure 2(c) shows a fluorescence image of the cells 24 h after the addition of virus. The intensity of fluorescence was proportional to the amount of E2 polypeptide in the cells. The images indicated that the virus proliferated in 5% to 10% of the cells that showed intense fluorescence emission. Weak fluorescence observed in other cells was probably due to a low concentration of the E2 polypeptide produced, suggesting that the virus had not proliferated in these cells.

Raman spectra of HEK293 without (a) and with (b) virus and their difference spectrum (c) are shown in Fig. 3. The spectra were measured 48 h after the virus addition. The spectra

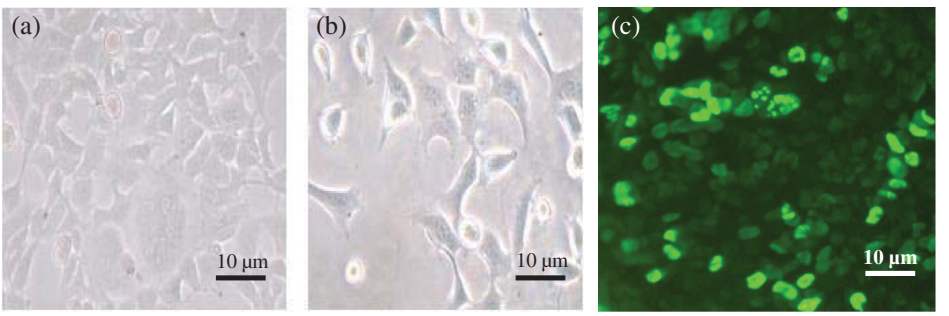

Fig. 2 Bright field images of HEK293 cells without (a; control) and with virus (b) 48 h after the virus addition. Fluorescence images of immunostained HEK293 cells with virus observed 24 h after virus addition (c).

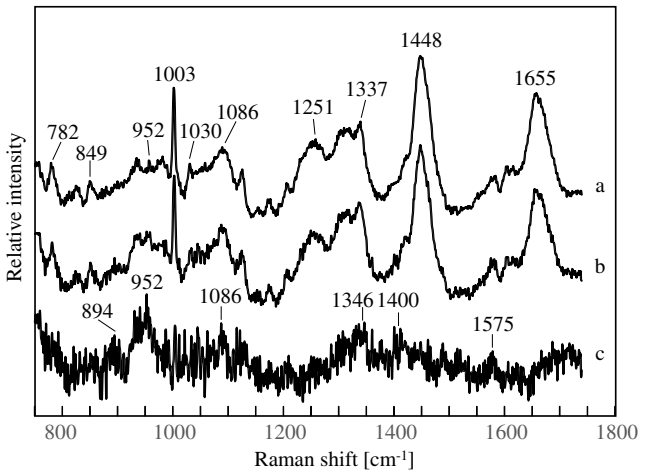

Fig. 3 Averaged Raman spectra of cells without (a) and with (b) virus, and their difference spectrum [(c); (a) and (b)].

measured 12 and 24 h after the virus addition are not shown, because characteristic differences were minimal. Bands at 1655, 1448, and 1337 cm^{-1} were assigned to amide I, CH bending, and amide III modes of proteins. A sharp band at 1003 cm^{-1} and a minor band at 1030 cm^{-1} were attributed to phenylalanine in the proteins. Bands at 1089 cm^{-1} were assigned to a symmetric stretching vibration mode of the phosphate and that at 850 cm^{-1} was assigned to DNA. These bands were clearly observed in the difference spectra, suggesting that the adenovirus infection significantly altered the concentration or composition of nuclear DNA.

The Raman spectra of control cells (without virus) were subjected to PCA (Fig. 4). Since we repeated the same experiments three times, the three datasets were expected to make a single distribution. As shown in the score plot [Fig. 4(A)], the datasets for different days formed independent groups, suggesting that the HEK293 cells were sensitive to subtle changes in the culture conditions, which could not be controlled. The loading plot [Fig. 4(B)] for PC 2 showed a strong contribution of free water near 1640 cm^{-1}. Therefore, the spectral region from 1550 to 750 cm^{-1} was selected for subsequent analysis to suppress the interference arising from changes in experimental conditions.

A score plot of PCA of the spectra of cells with and without virus 12 h after the addition of virus is shown in Fig. 5(a). Up to seven PCs were obtained and the PCA score plot was composed of two characteristic PCs with major differences between these two groups. The datasets of cells with and without virus showed significant differences. At the border area, some of the data from the virus-treated group overlapped with that of cells not treated with virus. These cells seemed not to sense the virus invasion yet. As described earlier, this data were collected from three independent experiments. When PCA was carried out for each experimental dataset, these three datasets highlighted consistent differences with high reproducibility. Loading plots for PC 1 are shown in Fig. 5(b). As the spectra were normalized with the band due to phenylalanine at 1003 cm^{-1}, the bands in the loading plot indicate relative changes to the concentration of phenylalanine. Bands at 1445 and 1302 cm^{-1} were observed in the positive direction, which may be attributed to changes in the composition of lipids. Bands at 1257, 1080, and 752 cm^{-1} were attributed to DNA. The PCA score plot for the spectra

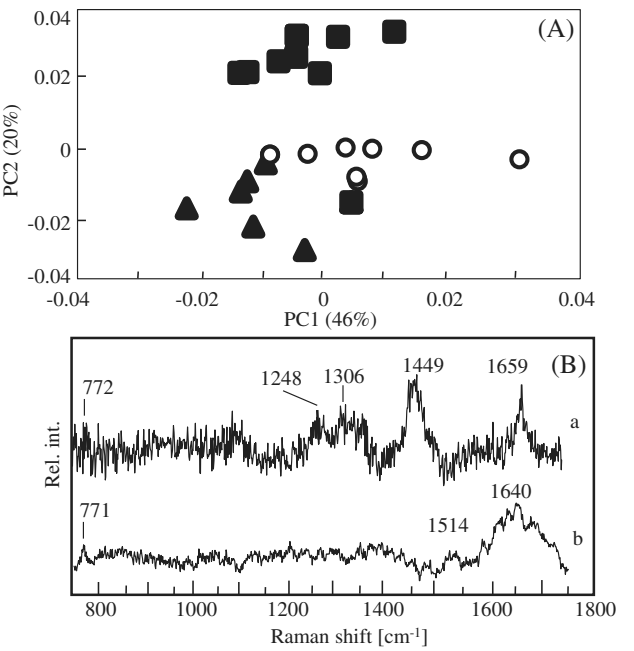

Fig. 4 Score plot (A) and loading plots (B) of principal component analysis (PCA) model constructed for the three control datasets collected 12 h after virus addition. The datasets obtained from the first (open circle), second (filled triangle), and third (filled square) experiments are plotted in the score plot for PC 1 and PC 2. The loading plots are depicted for PC 1 (a) and PC 2 (b).

recorded 24 h after the virus addition is shown in Fig. 6(A). PC 1 (not shown) was unrelated to viral infection and was probably due to variations in culture conditions. PC 2 contributed to the discrimination of two groups. Very few spectra of the cell-with-virus group were classified into the cell-without-virus group, suggesting that the virus infection progressed and

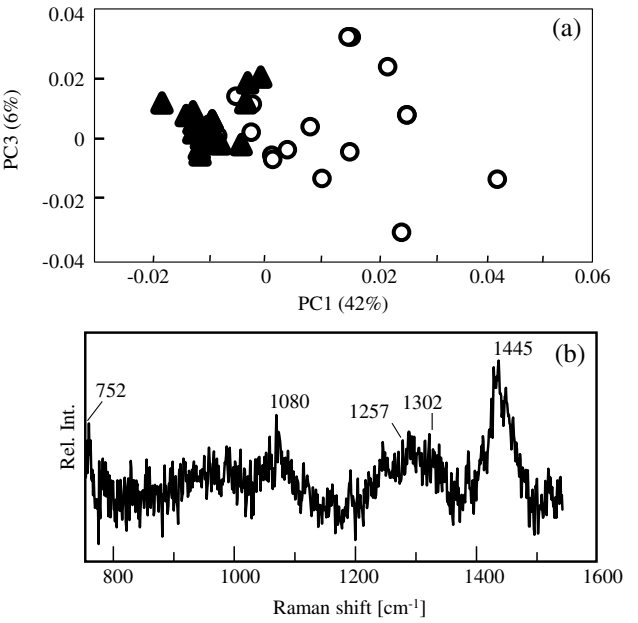

Fig. 5 Score plot (a) and loading plot (b) of PCA model constructed for the dataset collected 12 h after virus addition. The data from the control (open circle) and from a cell with the virus (filled triangle) are plotted in the score plot composed of PC 1 and PC 3. The loading plot is depicted for PC 1.

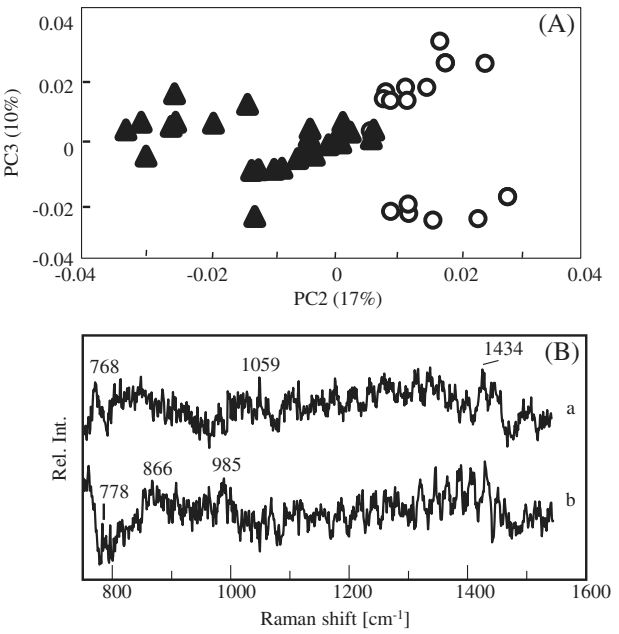

Fig. 6 Score plot (A) and loading plot (B) of PCA model constructed for the dataset collected 24 h after virus addition. The data from the control (open circle) and from a cell with the virus (filled triangle) are plotted in the score plot composed of PC 2 and PC 3. The loading plots are depicted for PC 2 (a) and PC 3 (b).

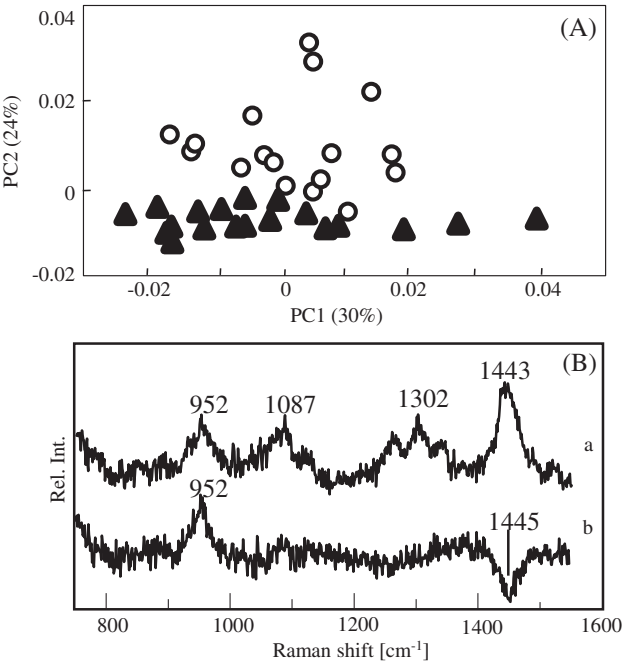

Fig. 7 Score plot (A) and loading plot (B) of PCA model constructed for the dataset collected 48 h after virus addition. The data for the control (open circle) and from a cell with the virus (filled triangle) are plotted in the score plot composed of PC 1 and PC 2. The loading plots are depicted for PC 1 (a) and PC 2 (b).

most of the cells had already sensed the virus invasion. The control (cell-without-virus) data separated into two groups along the PC 3 axis, which was attributed to the fluctuation of culturing conditions. The loading plot of PC 2 is shown in Fig. 6(B). The noisy nature of the plot suggested that the differences between spectra without and with virus were considerably small. A weak and broadband near 1434 cm^{-1}, which was almost buried in noise, was probably due to a CH bending mode. A positive band near 768 cm^{-1} was attributed to DNA. Bands at 985 and 866 cm^{-1}, observed in the positive direction in PC 3, were due to polysaccharides. The PCA score plot for spectra 48 h after the virus addition is shown in Fig. 7(A). The plot showed good discrimination between two groups within the PC 2 axis. There was some overlap between the two groups. The loading plot of PC 2 is shown in Fig. 7(B-b). A negative band near 1445 cm^{-1} was due to the CH bending mode. A positive band at 952 cm^{-1} does not have strong accompanying bands. This feature resembles the Raman spectrum of the PO_4^{3-} group and it may indicate that the normal uninfected cells had more Ca^{2+} ions than did the virus-infected cells. The features of the loading plots for the cells 12, 24, and 48 h after the virus addition were different, which appeared to reflect the dynamics of the reaction of the cells. During the early stages of infection (<12 h), several cells with virus were found to be classified into the group of cells without virus, because the virus had not yet succeeded in invading these cells. At 24 h, the overlap between the groups of cells with and without the virus was much smaller. It appears that the spectral changes reflected the self-defense reaction of the cells to the virus infection. As evident from the fluorescence images, in the cells, the virus started replicating 48 h after its addition. The noise level in PC 2 of the data collected 48 h after virus addition was much lower than those corresponding to data collected after 12 and 24 h, indicating a much larger spectral alteration. The analysis of fluorescence emission showed that 5% to 10% of the cells emitted intense fluorescence, whereas the Raman analysis classified nearly 100% of the cells into the infected group. Judging from the MOI (6 PFU/cell), six virus particles were used to infect one cell, a ratio sufficiently high to ensure that all cells are infected. Therefore, the Raman analysis was more sensitive in detecting the viral infection than the conventional fluorescence imaging methods.

4 Conclusion

The present study demonstrates that Raman spectroscopy can be used for sensitively detecting viral infections in live cells without any labeling. The viral infection was detected 12 h after incubating the cells with the virus. Further, the Raman spectroscopy is a faster method for the detection of viral infection than the conventional immunostaining method. The newly developed method does not require specific information on the virus for the analysis. The spectral changes observed 12 and 24 h after virus addition are probably due to the defense response of the cells to infection. The spectral changes observed 48 h after the addition of the virus were probably due to a combination of virus proliferation and defense response. The band at 952 cm^{-1} attributed to the PO_4^{3-} group was found to be a good marker for the proliferation of the virus in the cells.

Acknowledgments

This work was supported by supported by JSPS KAKENHI Grant Number 25560211.

References

1. E. Kastanos et al., "A novel method for bacterial UTI diagnosis using Raman spectroscopy," *Int. J. Spectrosc.* **2012**, 1–13 (2012).

2. P. C. Buijtels et al., "Rapid identification of mycobacteria by Raman spectroscopy," *J. Clin. Microbiol.* **46**(3), 961–965 (2008).
3. F. Jamal et al., "Raman spectroscopy of bacterial species and strains cultivated under reproducible conditions," *Spectroscopy* **27**(5–6), 361–365 (2012).
4. L. P. Maquelin et al., "Rapid identification of candida species by confocal Raman microspectroscopy," *J. Clin. Microbiol.* **40**(2), 594–600 (2002).
5. S. Meisel et al., "Raman spectroscopy as a potential tool for detection of Brucella spp. in milk," *Appl. Environ. Microbiol.* **78**(16), 5575–5583 (2012).
6. I. Notingher et al., "Application of FTIR and Raman spectroscopy to characterisation of bioactive materials and living cells," *Spectroscopy* **17**(2–3), 275–288 (2003).
7. Y. Oshima et al., "Discrimination analysis of human lung cancer cells associated with histological type and malignancy using Raman spectroscopy," *J. Biomed. Opt.* **15**(1), 017009 (2010).
8. K. Hartmann et al., "A study of Docetaxel- induced effects in MCF-7 cells by means of Raman microspectroscopy," *Anal. Bioanal. Chem.* **403**, 745–753 (2012).
9. J. M. Benevides et al., "Characterization of subunit-specific interactions in a double-stranded RNA virus: Raman difference spectroscopy of the phi6 procapsid," *Biochemistry* **41**(40), 11946–11953 (2002).
10. R. Tuma and G. J. Thomas, "Mechanisms of virus assembly probed by Raman spectroscopy: the icosahedral bacteriophage P22," *Biophys. Chem.* **68**(1–3), 17–31 (1997).
11. A. Schafer et al., "The latency-associated nuclear antigen homolog of herpesvirus saimiri inhibits lytic virus replication," *J. Virol.* **77**, 5911–5925 (2003).
12. E. Vargis et al., "Near-infrared Raman microspectroscopy detects high-risk human papillomaviruses," *Transl. Oncol.* **5**(3), 172–179 (2012).
13. M. Relhan, M. Heikenwalder, and U. Protzer, "Direct effects of hepatitis b virus-encoded proteins and chronic infection in liver cancer development," *Digest. Dis* **31**(1), 138–151 (2013).
14. W. S. M. William and A. E. Tollefson, "Adenovirus methods and protocols. Ad proteins, RNA, lifecycle, host interactionnetics, and phylogenetics," Chapter 21 in *Characterization of the Adenovirus Fiber Protein*, 2nd ed., Vol. 2, pp. 288–289, Humana Press, Totowa, New Jersey (2007).
15. J. A. Kramps et al., "A simple, specific, and highly sensitive blocking enzyme—linked immunosorbaent assay for detection of antibodies to bovine herpesvirus 1," *J. Clin. Microbiol.* **32**(9), 2175–2181 (1994).
16. K. E. Hamden et al., "Spectroscopic analysis of Kaposi's sarcoma-associated herpesvirus infected cells by Raman tweezers," *J. Virol. Methods* **129**, 145–151 (2005).
17. P. R. T. Jess et al., "Early detection of cervical neoplasia by Raman spectroscopy," *Int. J. Cancer* **121**, 2723–2728 (2007).
18. K. Ohtani et al., "Regulation of cell growth-dependent expression of mammalian CDC6 gene by the cell cycle transcription factor E2F," *J. Oncogene* **17**(14), 1777–1785 (1998).
19. M. P. Quinlan and T. Grodzicker, "Adenovirus E1A12S protein induces DNA synthesis and proliferation in primary epithelial cells in both the presence and absence of serum," *J. Virol.* **61**(3), 673–682 (1987).

Biographies for authors are not available.